JOURNAL OF MATERIALS SCIENCE **39** (2004) 3425–3432

The three-dimensional analysis for diffusive shrinkage of a grain-boundary void in stressed solid

HUA WANG, ZHONGHUA LI*
School of Civil Engineering and Mechanics, Shanghai Jiaotong University, 200240, Shanghai Minhang, People's Republic of China
E-mail: zhli@sjtu.edu.cn

As atoms migrate along void surface and grain-boundary driven by various thermodynamic forces, the grain-boundary void changes its shape and volume. A rounded void may become unstable and collapse. The void instability is an outcome of the competition between the variation in the elastic energy stored in the stressed solid, the void surface and grain-boundary energies. In this article, the instability conditions and the equilibrium shape of a gas-filled grain-boundary void are first determined, and then an explicit expression for the shrinkage rate is derived as a function of the void spacing, the applied stress, the internal pressure built up by the gas filled in the void as well as relevant material parameters.

1. Introduction

The polycrystalline materials used at elevated temperature tend to develop voids on the grain-boundaries, especially on those approximately normal to the applied stress. Their growth and coalescence lead to intergranular failure [1, 2]. The grain-boundaries form a continuous diffusion network for atoms [3]. Due to this fast diffusion path, the grain-boundary voids will shrink as atoms diffuse along the grain-boundaries into the voids [4]; or grow as atoms diffuse from the void surface into the grain-boundary [5]. The void growth or shrinkage on the planar bonding interface or on the planar grain-boundary interface was studied by many investigators [6, 7]. Some void shrinkage models [8–10] were developed from powder sintering models [11], and others [12, 13] were derived from void growth models [5, 14].

In the previous works, main attention has been paid to the rate of void growth (or shrinkage) under the assumption that the void maintains its spherical shape as it shrinks or grows [6, 15]. However, a rounded void can collapse into a crack by surface diffusion when the applied stress exceeds a critical value [16–20]. The final shape of a void within a grain is an outcome of the competition between the variation in the elastic energy stored in the solid and the surface energy [19, 20].

The situation becomes more complicated for grain-boundary voids. Experimental observations showed that the equilibrium shape of a grain-boundary void is a spheroid with elongation in grain-boundary, not a sphere [21]. Furthermore, as the grain-boundary void changes its shape and volume, the variation in the free energy of the system comes not only from the surface energy and the elastic energy stored in the solid, but also from the grain-boundary energy. The stable shape of a grain-boundary void, which has never been explored, would be a result of the competition between the variation in the elastic energy, the surface and grain-boundary energies.

The instability of a void within grain has been studied both in the case of volume-conserving [20] and in a rate of shrinkage and growing [22] for two-dimensional model, i.e., when the void is a cylindrical pore with rounded section. An explicit expression for the shrinkage rate has been obtained for the pore with a circular section [22], where the rate is controlled by lattice diffusion. However, the cylindrical pore is unstable. It tends to split into an array of discrete spheroidal voids *via* Rayleigh instability. Hence, the shape of a grain-boundary void observed by experiment is mostly in spheroidal state. Although the rate process between a void within a grain and a void on grain-boundary has some physical similarities, there is substantial difference between them: the former is controlled by grain-boundary diffusion while the latter by lattice diffusion. It is well known that the grain-boundary diffusion is several orders faster than the lattice diffusion. A quantitative estimation for evolving rate of a grain-boundary void is very desirable, because it is very important both in theory and practice as voids play a role in several important physical processes, such as diffusion bonding, powder sintering and damage healing [23].

Another concern is that the gas may diffuse into the void by some physical mechanisms. Experiments showed that the internal pressure built up by the gas

*Author to whom all correspondence should be addressed.

reduces the tendency for a void to collapse [21]. However, this has not been justified by any theoretical analysis.

In this article, we will first study the instability of a gas-filled grain-boundary void, and map out diverse evolving paths and identify the controlling parameters. Then an explicit expression for the shrinkage rate of a grain-boundary void will be derived. The analysis assumes that surface diffusion is sufficiently rapid compared to grain-boundary diffusion. Lattice diffusion and platicity are assumed to be negligible, so that only void surface and grain-boundary diffusions are the dissipative processes included in this analysis.

2. Energetics of an evolving grain-boundary void

Fig. 1 shows the three-dimensional model of a gas-filled oblate spheroidal void in infinite elastic solid. As diffusion varies the void, the solid varies its elastic field, the volume and shape of the void. Here an axisymmetric problem will be analyzed in which the void evolves as a sequence of oblate spheroids. The semi-axes of the void on the xy plane are equal under the remote triaxial stresses $\sigma_1 = \sigma_2 \leq \sigma_3$ and an internal pressure p, such that as diffusion changes the shape of the xz cross-section of the void, its shape in the xy cross-section maintains circle. Hence, the void can be represented by its xz cross-section.

2.1. The thermodynamic potential

The thermodynamic potential, consisting of elastic energy, void surface and grain-boundary energies, is a functional of the void shape, the void volume, the applied load and internal pressure p. The work done by the load either varies the energy in the solid, or produces entropy in the diffusion processes. The first law of thermodynamics requires that

$$(\text{energy rate}) + (\text{dissipation rate}) = (\text{work rate}) \quad (2.1)$$

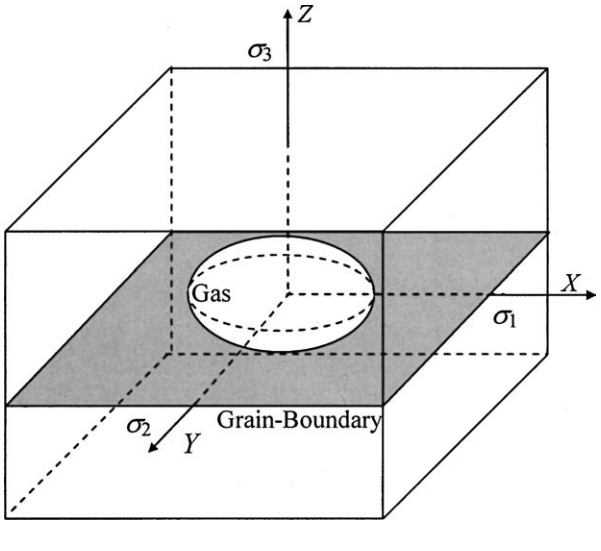

Figure 1 The schematic model of a gas-filled spheroidal void in elastic solid under triaxial stresses $\sigma_1 = \sigma_2 \leq \sigma_3$.

Denote w as the strain energy per volume, γ_s the surface energy per area on void surface and γ_b the energy per area on grain-boundary. They are taken to be independent from each other for practical purpose. The strain field in the body is determined by the elasticity theory neglecting the effect of interface energies. The total elastic energy and interface energies are

$$U_e = \int_{\text{body}} w \, dV, \; U_s = \int_{\text{surface}} \gamma_s \, dA_s,$$
$$U_b = \int_{\text{grain-boundary}} \gamma_b \, dA_b \quad (2.2)$$

Under the fixed mechanical load, the suitable potential is

$$\Phi = U_e + U_s + U_b - (\text{load} \times \text{displacement}) \quad (2.3)$$

Furthermore,

$$U_e = (\text{load} \times \text{displacement})/2 \quad (2.4)$$

for linear elastic solids. Thus, the thermodynamic potential for linear elastic solids under constant load is

$$\Phi = -U_e + U_s + U_b \quad (2.5)$$

For a given void, U_e is determined by the elasticity problem, U_s is integrated over the area of the void surface A_s and U_b over the area of the grain-boundary A_b.

Then (2.1) becomes

$$\frac{d\Phi}{dt} + (\text{dissipation rate}) = 0 \quad (2.6)$$

The second law of thermodynamics requires that the dissipation be positive as atoms diffuse. That is, atoms diffuse to reduce the potential of the system.

In the following, the difference of the potential energy between a spheroid and a sphere with radius ρ_0 is calculated, i.e.,

$$\Delta\Phi = \Phi(\text{spheroid}) - \Phi(\text{sphere}) \quad (2.7)$$

The shape of a spheroidal void having the same volume as a spherical one of radius ρ can be described by

$$X = Y = \rho\sqrt{\frac{1+m}{1-m}}\cos\theta \quad Z = \rho\frac{1-m}{1+m}\sin\theta \quad (2.8)$$

The spherical void corresponds to $m = 0$, the crack to $m \to 1$.

An infinite body containing a spheroidal void subjected to remote triaxial stresses and internal pressure, stores infinite amount of strain energy. Yet, the energy difference between a body containing a spheroidal void and a body without void subjected to the same stresses can be computed. The increase in strain energy upon introducing a spheroidal void to an infinite solid, U_e, can be formulated by following the method of Eshelby

[24] as

$$U_e = \frac{4\pi\rho^3(\sigma_3 + p)^2}{3E} A \tag{2.9}$$

where the dimensionless coefficient A, listed in Appendix, is a function of the shape parameter m, the stress ratio $\omega = (\sigma_1 + p)/(\sigma_3 + p)$ and the Poisson's ratio ν. σ_1 and σ_3 are positive for tensile stress and p is positive for compression. Thus, the elastic energy differs by

$$\Delta U_e = \frac{4\pi\rho_0^3(\sigma_3 + p)^2}{3E}(\alpha^3 A - A_0) \tag{2.10}$$

where $\alpha = \rho/\rho_0$, A_0 is A of a spherical void with radius ρ_0. The increase in the surface energy upon introducing a spheroidal void onto a grain-boundary is:

$$U_s = 4\pi\rho^2\gamma_s B \tag{2.11}$$

And the increase in the grain-boundary energy is:

$$U_b = -\pi\rho^2\gamma_b \frac{1+m}{1-m} \tag{2.12}$$

where the dimensionless number B, listed in Appendix, is a function of m. Thus, the interface energy differ by

$$\Delta U_s = 4\pi\rho_0^2\gamma_s(\alpha^2 B - 1) \tag{2.13}$$

$$\Delta U_b = \pi\rho_0^2\gamma_b\left(1 - \alpha^2\frac{1+m}{1-m}\right) \tag{2.14}$$

Combining (2.10), (2.13) and (2.14), the total difference in the potential is

$$\frac{\Delta\Phi}{4\pi\rho_0^2\gamma_s} = -\frac{\Lambda}{3}(\alpha^3 A - A_0) + (\alpha^2 B - 1) + \lambda\left(1 - \alpha^2\frac{1+m}{1-m}\right) \tag{2.15}$$

where $\lambda = \gamma_b/4\gamma_s$ is interface energy ratio; $\Lambda = (\sigma_3 + p)^2\rho_0/\gamma_s E$ is a dimensionless loading parameter that describes the relative importance of the elastic energy and the surface energy.

2.2. The critical value of Λ

As shown in (2.15), for a given Λ, Φ is a function of shape parameter m, volume parameter α, stress ratio ω and interface energy ratio λ. If $\alpha = 1$, $p = 0$ and $\lambda = 0$, corresponding to a vacuum void in a grain with constant volume, (2.15) returns to the results obtained by Sun *et al.* [20]. For the case of $\sigma_1 = \sigma_2 = \sigma_3$, a critical loading parameter $\Lambda_c = 16/9$ was obtained. If Λ exceeds the critical value Λ_c, a spherical void will collapse to a crack. For a grain-boundary void, the potential described by (2.15) is a complicated function of multi-parameter. To separately visualize the effect of α and λ on the critical value Λ_c and the equilibrium shape of the void, we first set $\omega = 1$ and $\lambda = 0$, corresponding to a void within a hydrostatically stressed grain. Then (2.15) reduces to

$$\frac{\Delta\Phi}{4\pi\rho_0^2\gamma_s} = -\frac{\Lambda}{3}(\alpha^3 A - A_0) + (\alpha^2 B - 1) \tag{2.16}$$

Expand (2.16) in powers of m

$$\frac{\Delta\Phi}{4\pi\rho_0^2\gamma_s} = \alpha^2 - 1 + \frac{1}{2}(1 - \alpha^3)\Lambda + (1.6\alpha^2 - 0.9\alpha^3\Lambda)m^2 + \cdots \tag{2.17}$$

Here only two leading terms are retained for small m. When $\Lambda > 16/(9\alpha)$, the coefficient is negative for m^2, so that $m = 0$ maximizes Φ. When $\Lambda < 16/(9\alpha)$, the coefficient is positive for m^2, so that $m = 0$ minimizes Φ. Consequently, $\Lambda = 16/(9\alpha)$ is the critical value Λ_c, below which the void keeps its spherical shape during shrinking or growing.

Then, we set $\omega = 1$ but $\lambda \neq 0$, corresponding a void located on grain-boundary. Fig. 2a displays the function Φ at several constant levels of $\alpha\Lambda$ for $\lambda = 1/11$ (data for pure iron with bcc lattice [25], $\gamma_s = 2.2$ J/m^2, $\gamma_b = 0.8$ J/m^2. Each minimum and maximum on the curves represents a stable and unstable equilibrium state, respectively. A critical value $\alpha\Lambda_c \approx 0.86$ can be sought by detailed numerical analyses. As shown in

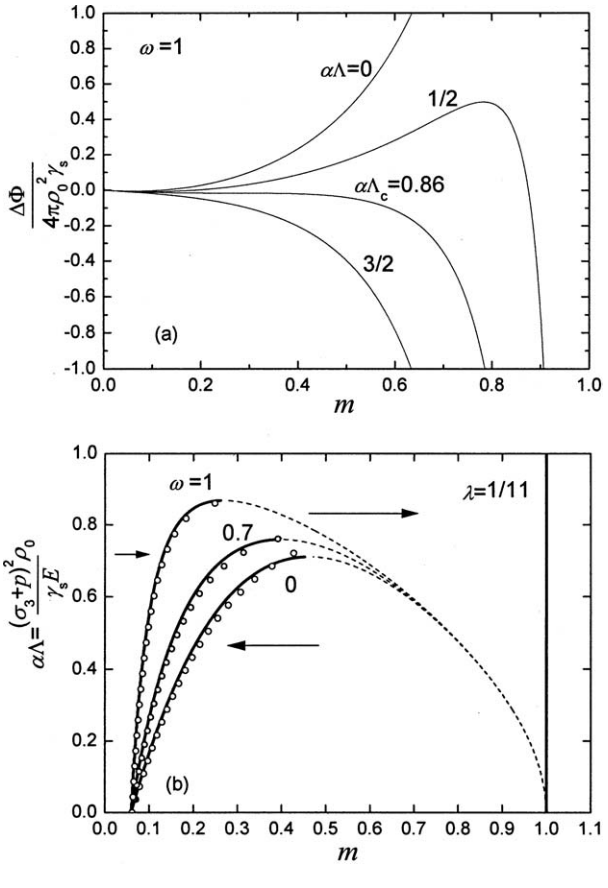

Figure 2 (a) The potential as a function of the void shape parameter m at several levels of $\alpha\Lambda$ for $\omega = 1$ and $\lambda = 1/11$. (b) Stability conditions projected on the $(m, \alpha\Lambda)$ plane. The heavy solid and dotted lines are the numerical solutions to the stable and unstable equilibrium shapes from (2.15); the hollow circles are the stable equilibrium shapes predicted by (2.23).

Fig. 2a:

1. when $\alpha\Lambda = 0$, the stress vanishes. Φ reaches a minimum at $m = m_e$, and two maxima at $m = 0$ and 1. Any void will relax to a spheroidal one of m_e.

2. when $\alpha\Lambda \in (0, \alpha\Lambda_c)$, the surface energy dominates. Φ reaches two maxima at $m = 0$ and m_c, and two minima at $m = m_e$ and 1. The maxima act as energy barrier: a void of $m < m_c$ will relax to that of m_e, but a void of $m > m_c$ will collapse to a crack.

3. when $\alpha\Lambda \in (\alpha\Lambda_c, \infty)$, the strain energy dominates; Φ reaches the maximum at $m = 0$, and minimum at $m = 1$. Any void will collapse to a crack.

The equilibrium states under several remote stress states are plotted in the $(\alpha\Lambda, m)$ space, as shown in Fig. 2b. The heavy solid and the dotted lines correspond to the stable and the unstable equilibrium states, respectively. The evolving direction in each region is indicated by an arrow. A void settles to a rounded shape when $\alpha\Lambda$ is small, but collapses to a crack when $\alpha\Lambda$ is large. $\alpha\Lambda$ reaches a critical value at the joint point of a heavy solid line and a dotted line.

Fig. 2 shows that the stable equilibrium shape of a grain-boundary void ($\lambda = 0$) is not a sphere, but a spheroid of m_e with elongation in the grain-boundary plane [21]. Both the critical value Λ_c and the equilibrium shape parameter m_e are a function of α, ω, λ. They should be determined before we discuss the shrinkage rate. Although they can be sought by detailed numerical analysis, it is not convenient for practice. An approximate expression for m_e and Λ_c can be obtained by expanding (2.15) in powers of m

$$\begin{aligned}\frac{\Delta\Phi}{4\pi\rho_0^2\gamma_s} &= -\frac{\Lambda\omega_1}{6}(1-\alpha^3) + (1-\alpha^2)(\lambda-1) \\ &\quad -(\alpha\Lambda\omega_2 + 2\lambda)\alpha^2 m + (1.6 - \alpha\Lambda\omega_3 - 2\lambda)\alpha^2 m^2 \\ &\quad +(0.76 - \alpha\Lambda\omega_4 - 2\lambda)\alpha^2 m^3 + \cdots \end{aligned} \tag{2.18}$$

where

$$\left.\begin{aligned}\omega_1 &= 2 - 2\omega + 3\omega^2 \\ \omega_2 &= 0.57 - 0.14\omega - 0.43\omega^2 \\ \omega_3 &= 0.88 + 0.135\omega - 0.11\omega^2 \\ \omega_4 &= 1 + 0.1\omega + 0.43\omega^2\end{aligned}\right\} \tag{2.19}$$

only three leading terms of m are retained for small m. Equilibrium requires that $\partial\Phi/\partial m = 0$, i.e.,

$$\begin{aligned}&(\alpha\Lambda\omega_2 + 2\lambda) - 2(1.6 - \alpha\Lambda\omega_3 - 2\lambda)m \\ &\quad -3(0.76 - \alpha\Lambda\omega_4 - 2\lambda)m^2 = 0\end{aligned} \tag{2.20}$$

The critical value Λ_c can be solved from the discriminant of (2.20) and expressed by

$$\Lambda_c \approx \frac{\omega_5 + \omega_6\lambda - (\omega_7 + \omega_8\lambda + \omega_9\lambda^2)^{1/2}}{\alpha\omega_{10}} + \omega_{11} \tag{2.21}$$

$$\left.\begin{aligned}\omega_5 &= 2.991 + 1.5151\omega + 1.254\omega^2 \\ \omega_6 &= 11.959 - 1.55\omega + 0.9\omega^2 \\ \omega_7 &= 48.386 - 11.042\omega - 7.75\omega^2 \\ &\quad -7.79\omega^3 - 21.6\omega^4 \\ \omega_8 &= 43.367 + 41.32\omega + 43.245\omega^2 \\ &\quad +7.3\omega^3 + 18.8\omega^4 \\ \omega_9 &= 19.8 + 25.75\omega + 78.9\omega^2 \\ &\quad +34\omega^3 + 73\omega^4 \\ \omega_{10} &= -3.84153 + 1.96341\omega + 1.714\omega^2 \\ &\quad +1.151\omega^3 + 2.263\omega^4 \\ \omega_{11} &= -0.12013 + 0.7652\omega + 0.22715\omega^2 \\ &\quad -0.17983\omega^3\end{aligned}\right\} \tag{2.22}$$

where ω_{11} is introduced to correct the error caused by the truncation of the expansion of (2.15). The equilibrium state parameter m_e is

$$m_e = \frac{1.6 - 2\lambda + \alpha\Lambda\omega_{12} + (\lambda_1 + \alpha\Lambda\omega_{13} + \alpha^2\Lambda^2\omega_{14} + \alpha\Lambda\lambda\omega_{15})^{1/2}}{6\lambda - 2.2857 + 3\alpha\Lambda\omega_4} \tag{2.23}$$

$$\left.\begin{aligned}\lambda_1 &= 2.56 - 1.828\lambda - 8\lambda^2 \\ \omega_{12} &= -0.8755 - 0.1347\omega + 0.1102\omega^2 \\ \omega_{13} &= -1.4955 - 0.7576\omega - 0.627\omega^2 \\ \omega_{14} &= 0.936 + 0.491\omega + 0.428\omega^2 \\ &\quad +0.288\omega^3 + 0.5658\omega^4 \\ \omega_{15} &= -5.98 + 0.7752\omega - 0.453\omega^2\end{aligned}\right\} \tag{2.24}$$

As shown in Fig. 2b, the stable equilibrium shape parameter predicted from (2.23) has an acceptable accuracy to the numerical solution to (2.15).

Fig. 3 compares $\alpha\Lambda_c$ predicted from (2.21) with the numerical solution to (2.15). Excellent agreement can be found. Once the critical value is obtained from (2.21), the critical applied stress can be calculated by using $\Lambda_c = (\sigma_3 + p)^2\rho_0/\gamma_s E$. The critical compressive stress will increase and the critical tensile stress will decrease if $p > 0$. So, the internal pressure will reduce the tendency for the void to collapse under compressive applied stress as argued by Gittins [21] and increase it under tensile applied stress.

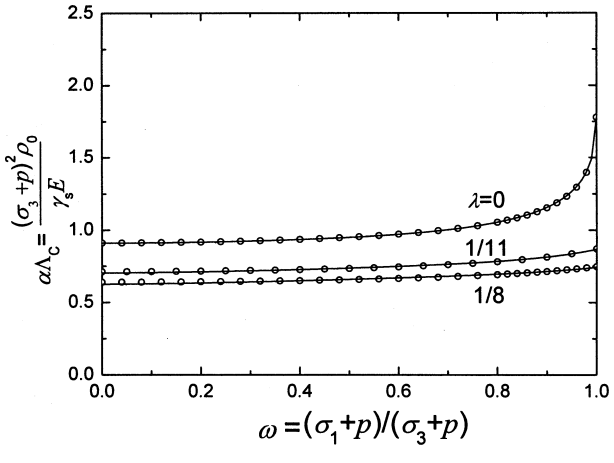

Figure 3 The comparison between the critical value $\alpha\Lambda_c$. The solid line is calculated by using (2.21); and the hollow circles are the numerical solution to (2.15).

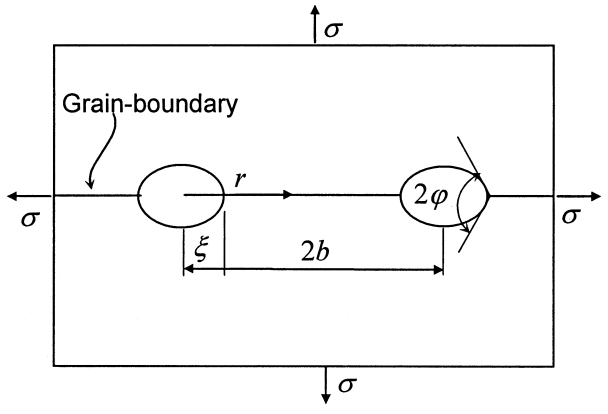

Figure 4 The schematic model for an array of gas-filled voids on a planar grain-boundary under hydrostatic pressure.

3. Kinetics of the grain-boundary void shrinkage by diffusion

In this section, we will derive the shrinkage rate of an array of gas-filled grain-boundary voids located under hydrostatic pressure $\sigma_1 = \sigma_2 = \sigma_3 = \sigma$. The initial radius of the void is ρ_0, and the void spacing is $2b$ as shown in Fig. 4. Let r be the distance along the grain-boundary to the center of a void. It should be noted that the basic Equation 2.15 is strictly valid only for an infinite solid containing a single void. For the model shown in Fig. 4, it can be approximatley used if the initial size of the void is small enough compared to the void spacing.

The excess chemical potential on the grain-boundary is

$$\Delta\mu = -\sigma_{\mathrm{n}}(r)\Omega \tag{3.1}$$

where $\sigma_{\mathrm{n}}(r)$ is the net normal stress acting on the grain-boundary, positive for tensile stress; Ω the atomic volume.

The atom flux J along the grain-boundary is

$$J = -\frac{D_{\mathrm{b}}\delta_{\mathrm{b}}}{kT\Omega}\nabla(\Delta\mu) \tag{3.2}$$

where D_{b} is the grain-boundary diffusion coefficient (assumed to be isotropic), δ_{b} the grain-boundary thickness, k Boltzmann's constant and T the absolute temperature.

When the applied stress is static, the grain-boundary diffusion can be taken to be in a steady state, which is [26, 27]

$$divJ = \eta \tag{3.3}$$

where η is the number of atoms removed per unit time and per unit volume from the grain-boundary, independent of r because of the steady state.

Substituting (3.2) into (3.3), we obtain the differential equation

$$\nabla^2(\Delta\mu) + \frac{\eta kT\Omega}{D_{\mathrm{b}}\delta_{\mathrm{b}}} = 0 \tag{3.4}$$

The appropriate solution to the distribution of excess chemical potential on the grain-boundary is

$$\Delta\mu = C_1 r^2 + C_2 + C_3 \ln r \tag{3.5}$$

where $C_1 = -kT\Omega\eta/4D_{\mathrm{b}}\delta_{\mathrm{b}}$, C_2 and C_3 are constants to be determined by the following boundary conditions.

Firstly, the excess chemical potential $\Delta\mu$ on the void surface can be expressed as

$$\Delta\mu_{\mathrm{s}} = -\gamma_{\mathrm{s}}(\kappa_{\mathrm{xz}} + \kappa_{\mathrm{xy}})\Omega + w \tag{3.6}$$

where κ_{xz}, κ_{xy} are the principal curvatures on xz and xy planes, taken to be positive for a convex surface. In a material capable of matter transport by diffusion, $\Delta\mu$ must be continuous at the void apex ($r = \xi$) where it meets the grain-boundary. Rice and Chuang [28] proved that the strain energy terms could be neglected because grain-boundary diffusion effectively alleviates the stress concentration at the void apex. So the excess chemical potential at the void apex is given by

$$\Delta\mu_{\mathrm{s}}(r = \xi) = -\gamma_{\mathrm{s}}(\kappa_{\mathrm{xz}} + \kappa_{\mathrm{xy}})\Omega \tag{3.7}$$

For the spheroidal void described by m_{e}, the curvature at the void apex, $r = \xi = \rho\tau^{1/2}$, is

$$\kappa_{\mathrm{apex}} = -(\kappa_{\mathrm{xz}} + \kappa_{\mathrm{xy}}) = -\frac{\tau^3 + 1}{\rho\tau^{1/2}}, \quad \tau = \frac{1 + m_{\mathrm{e}}}{1 - m_{\mathrm{e}}} \tag{3.8}$$

Thus, the continuous condition in the excess chemical potential at the void apex is:

$$-\Omega\sigma_{\mathrm{n}}(r = \xi) = \frac{-\gamma_{\mathrm{s}}\Omega(\tau^3 + 1)}{\rho\tau^{1/2}} \tag{3.9}$$

Secondly, because of symmetry, the matter flux vanishes at $r = b$. So we have

$$(\partial\Delta\mu/\partial r)_{r=b} = 0 \tag{3.10}$$

Finally, the condition of mechanical balance is

$$\int_{\xi}^{b} \frac{\Delta\mu}{\Omega} 2\pi r\,\mathrm{d}r = \int_{\xi}^{b} -\sigma_n(r)2\pi r\,\mathrm{d}r = -\pi b^2\sigma - \pi\xi^2 p \tag{3.11}$$

We assume that the gas could not leak away from the void. As the void shrinks, the initial pressure p_0 will be enlarged by the decrement of void volume. Assuming ideal gas behavior, so $p = p_0/\alpha^3$.

Note that the equilibrium angle $\cos\varphi = \gamma_{\mathrm{b}}/2\gamma_{\mathrm{s}}$ at the apex of a grain-boundary void (see Fig. 4) can be satisfied only when the gradient in excess chemical potential along the void surface and grain-boundary is quite small. The true equilibrium state is satisfied only if no atom flux occurs. However, the diffusion process discussed here is essentially dynamic, which may change the dihedral angle from the equilibrium one [27]. We can, therefore, examine the void shrinkage in the case where the dihedral angel can freely change.

The removal of atoms from the grain-boundary to the void causes adjacent grains to move close at a rate $\eta\Omega$ [27], thus, decreases the void volume at a rate $\pi\xi^2\,\eta\Omega$. This term is important when the void size is comparable with the void spacing [29]. The collection of atoms further decreases the void volume at a rate $\pi(b^2-\xi^2)\eta\Omega$. So the total shrinkage rate of the voids can be given as

$$\frac{\mathrm{d}V}{\mathrm{d}t} = -\eta\pi b^2\Omega \tag{3.12}$$

Solve the differential Equation 3.5 subjected to the boundary conditions (3.9)–(3.11), we obtain the number η

$$\eta = \frac{8D_\mathrm{b}\delta_\mathrm{b}\gamma_\mathrm{s}}{kTb^2\rho\sqrt{\tau}}\,\frac{\rho\sigma\sqrt{\tau}/\gamma_\mathrm{s} + x^2\rho p_0\tau^{3/2}/(\alpha^3\gamma_\mathrm{s}) - (1+\tau^3)(1-x^2\tau)}{[3-4x^2\tau+x^4\tau^2+4\ln(x\sqrt{\tau})]} \tag{3.13}$$

where $x = \rho/b$. Thus, the shrinkage rate of the voids is obtained from (3.12)

$$\frac{\mathrm{d}\rho}{\mathrm{d}t} = -\Omega\eta/4x^2 \tag{3.14}$$

(3.14) exhibits the dependence of the void shrinkage rate on the applied stress, the internal pressure, the ratio ρ/b, τ (related to shape parameter m_e) and the material parameters related to surface and grain-boundary diffusions.

Defining the normalized shrinkage rate as

$$\begin{aligned}\frac{\mathrm{d}\rho^*}{\mathrm{d}t} &= \frac{\mathrm{d}\rho}{\mathrm{d}t}\,\frac{kTb^3}{2D_\mathrm{b}\delta_\mathrm{b}\gamma_\mathrm{s}\Omega} \\ &= -\frac{\rho\sigma\sqrt{\tau}/\gamma_\mathrm{s} + x^2\rho p_0\tau^{3/2}/(\alpha^3\gamma_\mathrm{s}) - (1+\tau^3)(1-x^2\tau)}{x^3\sqrt{\tau}[3-4x^2\tau+x^4\tau^2+4\ln(x\sqrt{\tau})]}\end{aligned} \tag{3.15}$$

4. Examples and discussion

In this section, we examine the shrinkage behavior for an array of grain-boundary voids at temperature $T = 973$ K by using (3.15). The initial radius $\rho_0 = 2\ \mu$m and the void spacing $2b = 40\ \mu$m. The relevant material parameters for a pure iron with bcc lattice (α-Fe) are: $\gamma_\mathrm{s} = 2.2$ J/m^2, $\gamma_\mathrm{b} = 0.8$ J/m^2, $E = 2.1\times10^{11}$ N/m^2, $\delta_\mathrm{b} = 4.96\times10^{-10}$ m, $D_\mathrm{b} = 3.52\times10^{-12}$ m^2/s [25, 29].

The interface energy ratio $\lambda = \gamma_\mathrm{b}/4\gamma_\mathrm{s} = 1/11$. The critical Λ_c calculated from (2.21) is 0.86 for the initial void. So the critical compressive stress $\sigma_\mathrm{c} = -\sqrt{0.86\gamma_\mathrm{s}E/\rho_0} = -478$ MPa. The stable equilibrium shape parameter m_e is calculated from (2.23).

Fig. 5 shows the normalized shrinkage rate of a gas-free void at different external pressure levels. Under fixed external pressure, the void shrinkage rate increases monotonously as the voids become small. The void shrinkage rate can be accelerated as the external pressure increases.

The influence of the internal pressure p_0 on the void shrinkage rate is shown in Fig. 6. The shrinkage rate first increases, then decreases until the void stops shrinking as it becomes so small that the internal pressure becomes high enough. Therefore, the gas-filled grain-boundary voids cannot be eliminated. Residual voids will inevitably exist even when a higher hydrostatic pressure is applied. It is also imagined that if the applied pressure is reduced, the residual voids will grow up to a certain degree.

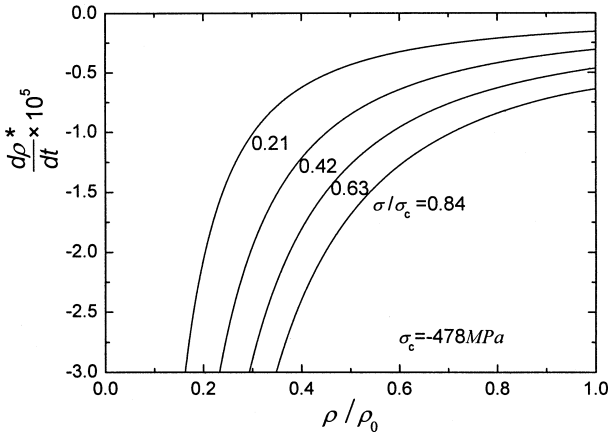

Figure 5 The normalized shrinkage rate for a gas-free grain-boundary void under hydrostatic pressure.

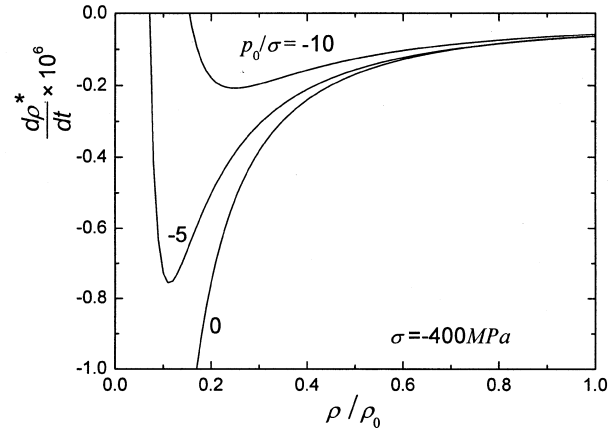

Figure 6 The influence of internal pressure p_0 on the shrinkage rate of the grain-boundary void.

Fig. 7 shows the relative dependence of the shrinkage rate on the void spacing $2b$. The rate decreases significantly with increasing void spacing. The results are well matched with that the growth rate of the voids is approximately inversely proportional to the void spacing for a purely diffusive creep [29]. Hence, void spacing is one of the important factors that control the shrinkage rate of the grain-boundary voids.

Integrating (3.15) numerically, we can obtain the time spent by void healing. As shown in Fig. 5, the vacuum void can be completely healed under hydrostatic pressure. The time needed to completely heal the gas-free void is displayed in Fig. 8, which deceases as the hydrostatic pressure increases. However, as shown in Fig. 9, the healing time for the gas-filled grain-boundary void increases infinitely when the void shrinkage rate vanishes eventually.

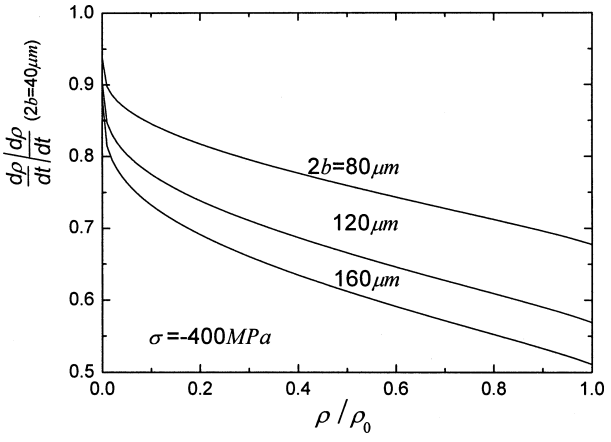

Figure 7 The relative dependence of the shrinkage rate on various void spacings.

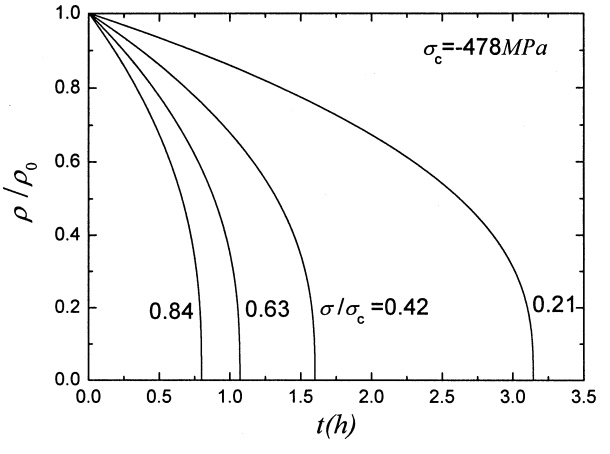

Figure 8 The healing time for the gas-free grain-boundary void at several external pressure levels.

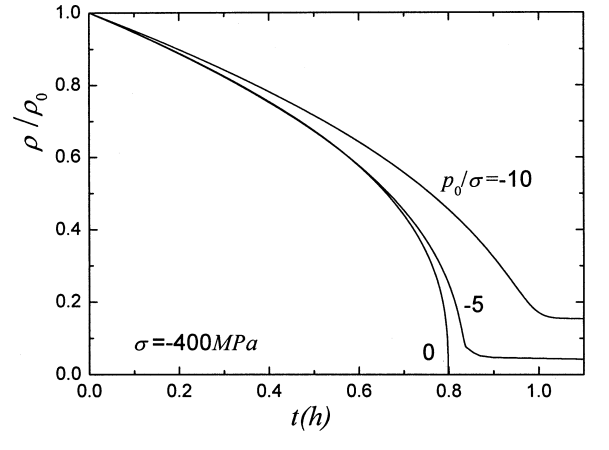

Figure 9 The healing time for the gas-filled grain-boundary void at different internal pressure levels.

5. Conclusions

A suitable thermodynamic potential has been established, from which the critical bifurcation condition and the stable equilibrium shape of a grain-boundary void in stressed solid are obtained. Based on the kinetic law, the shrinkage rate of the void is also derived. Some important results are:

1. High external pressure may effectively accelerate the shrinkage rate of the void. However, the load must be kept to be less than critical value to maintain a stable shape; otherwise the void will collapse.

2. Void on grain-boundaries cannot maintain a spherical shape, even if stressed hydrostatically. The void changes its shape continuously as it evolves to its equilibrium shape.

3. The gas-free voids could be totally eliminated. For a close gas-filled void, the internal pressure increases as the void shrinks. The pressure will retard the shrinkage rate, and eventually stop the shrinkage process as it becomes high enough. The shrinkage rate is significantly affected by the void spacing, increasing with decreasing void spacing.

Appendix

The increase of the strain energy upon introducing a gas-filled spheroidal void into an infinite solid was computed by following the method of Eshelby [24]. The coefficient in (2.9) is

$$A = (2\omega^2 C_{11} + 2\omega C_{13} + \omega C_{31} + C_{33})/2 \qquad (1)$$

where $\omega = (p + \sigma_1)/(p + \sigma_3)$, and

$$\left.\begin{aligned} C_{11} &= [(1 - S_{11})(1 - \nu) - 2\nu S_{13}]/\Delta \\ C_{13} &= [S_{13} - (1 - S_{33})\nu]/\Delta \\ C_{31} &= [2S_{31}(1 - \nu) - 2\nu(1 - S_{11} - S_{12})]/\Delta \\ C_{33} &= (1 - S_{11} - S_{12} - 2\nu S_{31})/\Delta \\ \Delta &= (1 - S_{33})(1 - S_{11} - S_{12}) - 2S_{31}S_{13} \end{aligned}\right\} \qquad (2)$$

all S_{ij} can be found in Eshelby [24].

The surface energy was calculated by integrating the surface tension over the spheroid surface. The coefficient in (2.11) is

$$B = \frac{\varsigma^2}{2} + \frac{\ln(\sqrt{\varsigma^6 - 1} + \varsigma^3)}{2\varsigma\sqrt{\varsigma^6 - 1}} \qquad (3)$$

where $\varsigma = \sqrt{(1 + m)/(1 - m)}$.

Acknowledgment

The financial support from the National Science Foundation of China under grant No. 10272705 is gratefully acknowledged.

References

1. A. C. F. COCKS and A. A. SEARLE, *Acta Metall. Mater.* **38** (1990) 2493.
2. V. SKLENIČKA, *Mater. Sci. Eng.* A **234–236** (1997) 30.
3. H. P. LONGWORTH and C. V. THOMPSON, *Appl. Phys. Lett.* **60** (1992) 2219.
4. H. H. YU and Z. SUO, *J. Mech. Phys. Solid.* **47** (1999) 1131.
5. T. J. CHUANG, K. I. KAGAWA, J. R. RICE and L. B. SILLS, *Acta Metal.* **27** (1979) 265.
6. M. V. SPEIGHT and W. BEERE, *Met. Sci.* **9** (1975) 190.
7. Y. TAKAHASHI and K. INOUE, *Sci. Technol.* **8** (1992) 953.
8. B. DERBY and E. R. WALLACH, *Met. Sci.* **16** (1982) 49.
9. A. HILL and E. R. WALLACH, *Acta Metall.* **37** (1989) 2425.

10. E. ARZT and K. E. EASTERLING, *Metall. Trans.* **14A** (1983) 211.
11. Y. TAKAHASHI, F. UENO and K. NISHIGUCHI, *Acta Metall.* **36**(11) (1988) 3007.
12. Z. X. GUO and N. RIDLEY, *Mater. Sci. Technol.* **3** (1987) 945.
13. J. W. HANCOCK, *Met. Sci.* **10** (1976) 319.
14. M. V. SPEIGHT and J. E. HARRIS, *ibid.* **1** (1967) 83.
15. H. E. EVANS and G. K. WALKER, *ibid.* **4** (1970) 210.
16. L. N. MCCARTNEY, *Acta Metall.* **25** (1997) 221.
17. H. GAO, *Q. J. Mech. Appl. Math.* **45** (1992) 149.
18. *Idem.*, *Proc. Roy. Soc. Lond.* **448** (1995) 465.
19. Z. SUO and W. WANG, *J. Appl. Phys.* **76** (1994) 3410.
20. B. SUN, Z. SUO and A. G. EVANS, *J. Mech. Phys. Solid.* **42** (1994) 1653.
21. A. GITTINS, *Acta Metall.* **16** (1968) 517.
22. H. WANG and Z. LI, *J. Mech. Phys. Solid,* **51** (2003) 961.
23. P. HUANG, Z. LI and J. SUN, *Metall. Mater. Trans.* A **33A** (2002) 1117.
24. J. D. ESHELBY, *Proc. R. Soc. Lond.* A **241** (1957) 376.
25. J. W. MARTIN and R. D. DOBERTY, "Stability of Microstructure in Metallic System" (Cambridge University Press, 1976) p. 178.
26. R. RAJ and M. F. ASHBY, *Acta Metall.* **23** (1975) 653.
27. Y. TAKAHASHI, K. TAKAHASHI and K. NISHIGUCHI, *Acta Metall. Mater.* **39**(12) (1991) 3199.
28. J. R. RICE and T. CHUANG, *J. Amer. Ceram. Soc.* **64** (1981) 46.
29. W. BEERE and M. V. SPEIGHT, *Met. Sci.* **12** (1978) 172.

Received 19 September 2002
and accepted 3 February 2004